

## Article

# Transient and Quasi-Steady-State Analytical Methods for Simulating a Vertical Gas Flow in a Landfill with Layered Municipal Solid Waste

Xun Wu <sup>1,2,\*</sup> , Jianyong Shi <sup>2</sup>, Tao Zhang <sup>3</sup>, Yuping Li <sup>2</sup> and Shi Shu <sup>2</sup><sup>1</sup> College of Mechanics and Materials, Hohai University, Nanjing 211100, China<sup>2</sup> Geotechnical Engineering Research Institute, Hohai University, Nanjing 210024, China<sup>3</sup> School of Civil Engineering and Architecture, Nanchang Hangkong University, Nanchang 330063, China

\* Correspondence: wuxun@hhu.edu.cn

**Abstract:** The exploration of gas pressure and its distribution in landfills is a principal concern for the design and management of municipal solid waste (MSW) landfills. A one-dimensional analytical model was proposed to simulate a vertical gas flow in a landfill with layered MSWs. The transient analytical solution was obtained by the method of superposition and eigenfunction expansion and verified by a semi-analytical solution and numerical simulation. According to the results of a parametric analysis by the transient analytical solution, a vertical gas flow in landfills can be simplified to a quasi-steady-state flow. A quasi-steady-state analytical solution for simulating a vertical gas flow in a landfill with layered MSW is proposed. The quasi-steady-state analytical solution showed good agreement with the transient solution. Both temporal and spatial variations of the gas generation rate in MSW landfills were considered in the transient and quasi-steady-state analytical methods. A comparison between the proposed quasi-steady-state solution and the previously described steady-state solution showed that using the average gas generation rate or the gas generation rate corresponding to the average age of the MSW layer in the steady-state solution resulted in an error in the estimation of the gas pressure in landfills. The proposed solutions are reliable and can provide a reference for the design, management, and subsequent restoration of landfills.

**Keywords:** municipal solid waste; landfill gas; gas pressure; analytical solution; layered; gas generation

**MSC:** 34B60; 35K20



**Citation:** Wu, X.; Shi, J.; Zhang, T.; Li, Y.; Shu, S. Transient and Quasi-Steady-State Analytical Methods for Simulating a Vertical Gas Flow in a Landfill with Layered Municipal Solid Waste. *Mathematics* **2022**, *10*, 3658. <https://doi.org/10.3390/math10193658>

Academic Editor: Aleksandr Rakhmangulov

Received: 14 August 2022

Accepted: 29 September 2022

Published: 6 October 2022

**Publisher's Note:** MDPI stays neutral with regard to jurisdictional claims in published maps and institutional affiliations.



**Copyright:** © 2022 by the authors. Licensee MDPI, Basel, Switzerland. This article is an open access article distributed under the terms and conditions of the Creative Commons Attribution (CC BY) license (<https://creativecommons.org/licenses/by/4.0/>).

## 1. Introduction

Gas is generated through the degradation of organic components in municipal solid waste (MSW) landfills. The landfill gas typically consists of 50–60% (*v/v*) methane (CH<sub>4</sub>), 40–50% (*v/v*) carbon dioxide (CO<sub>2</sub>) and small quantities of sulphur dioxide and volatile organic compounds [1,2]. The escape of landfill gas into the atmosphere has adverse environmental impacts and causes health hazards [3–5]. Additionally, a high gas pressure might lead to the instability of the landfill [6,7]. Thus, a good understanding of the vertical gas flow in landfills has become a principal concern for the design and management of MSW landfills.

Numerous researchers have developed analytical methods to simulate the vertical gas flow in MSW landfills. Townsend et al. [8] proposed an analytical solution for a steady-state one-dimensional gas flow in landfills with horizontal collection systems. Li et al. [9] presented a one-dimensional transient analytical solution for gas pressure profiles in an MSW layer. Zeng et al. [10] developed a gas–solid coupling model to simulate gas migration in landfills. To simplify the solving process, the landfills considered in these studies were assumed to be homogeneous.

A typical landfill is usually deposited in layers and requires decades to be filled. During the construction of a new layer, degradation is already undergoing in the old MSW [11,12]. Air permeability and gas generation in the old waste are much different from those in the new layer [13,14]. The layered characteristics of MSW have been considered in some numerical models of gas migration in landfills. Jung et al. [15] proposed two-dimensional transient numerical models for the advective and diffusive flow of multiple gas components in a landfill with layered MSW. Hettiarachchi et al. [16] developed a one-dimensional transient numerical model to predict the settlement and gas pressures in a bioreactor landfill with layered MSW. Zhang et al. [17] established a one-dimensional transient numerical model to predict the gas pressure distribution in a landfill with layered new and old MSW. Xie et al. [18] proposed a transient dual-porosity model to analyse the gas pressure distribution in a layered landfill. Although the numerical methods can consider the layered properties of landfills, analytical methods are more efficient for a preliminary design and can offer fundamental insights into physical mechanisms. Therefore, this paper focused on an analytical model of gas flow in a landfill with layered MSW.

Yu et al. [19] presented a one-dimensional semi-analytical model for the vertical gas flow in a landfill with layered MSW. The solution was obtained in Laplace transform, and a numerical method was used to perform the inversion of the Laplace transform. The spatial variability of the gas generation rate in each MSW layer was not considered. Li et al. [20] presented a one-dimensional analytical model for the vertical gas flow in a landfill with layered MSW. Feng et al. presented a two-dimensional [21] and an axisymmetric [22] analytical model to analyse the vertical gas flow in a landfill with layered MSW. The gas flow in these studies was assumed to be a steady-state flow. The gas generation rate in each MSW layer was simplified to be constant. However, the time- and depth-dependent quantitative estimation of gas generation rate has been reported in numerous studies [23–25]. To the authors' knowledge, there are no analytical solutions for the vertical gas flow in a landfill with layered MSW considering the temporal and spatial variability of the gas generation rate.

The main objective of this study was to propose an analytical method for simulating the vertical gas flow in a landfill with layered MSW. Temporal and spatial variations of the gas generation rate in the MSW were considered. Firstly, a transient analytical solution was obtained. As a simplification, a quasi-steady-state analytical solution was proposed. The efficiency of the presented quasi-steady-state solution was verified by comparison with the transient analytical solution and an existing steady-state solution. The work represents a small but important advance that considers the temporal and spatial variability of gas generation for the design of MSW landfills.

## 2. Model Development

The assumptions made to derive the mathematical formulation are:

- (1) The landfill gas was assumed to be an equimolar mixture of CH<sub>4</sub> and CO<sub>2</sub> and considered to behave as an ideal gas [23];
- (2) Darcy's law was applied to the gas flow, and gas diffusion was not considered [23];
- (3) No external load was applied on the landfill, and the vertical stress with respect to the change of time was equal to zero [26];
- (4) The gas flow rate was much greater than the liquid flow rate in the landfill, and the influence of the pore liquid pressure on the gas pressure was neglected [26].

The vertical flow of gas in landfills, as illustrated in Figure 1, was considered. The mass balance equation for a gas in a unit cell of MSW is

$$\frac{1}{V_0} \frac{\partial M_a}{\partial t} = -\frac{\partial(\rho_a v_z)}{\partial z} + q_a \quad (1)$$

where  $V_0$  is the volume of the unit cell ( $\text{m}^3$ );  $M_a$  is the gas mass in the unit cell (kg);  $\rho_a$  is the gas density ( $\text{kg}\cdot\text{m}^{-3}$ );  $v_z$  is the vertical flow velocity of the gas ( $\text{m}\cdot\text{s}^{-1}$ );  $q_a$  is the gas generation rate due to the degradation of MSW ( $\text{kg}\cdot\text{m}^{-3}\cdot\text{s}^{-1}$ ).

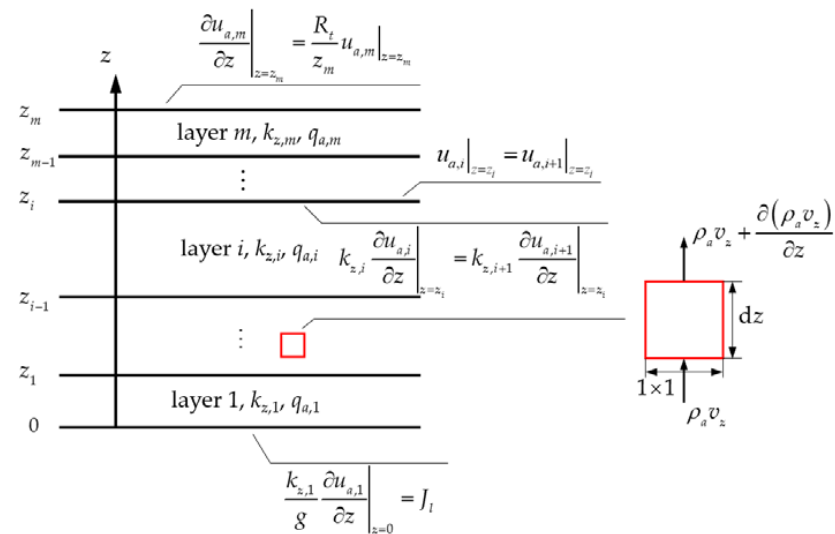


**Figure 1.** Schematic diagram of the vertical gas flow in a landfill with layered MSW (red rectangle represents a unit of MSW).

The first-order decomposition rate model is widely used to predict gas generation in landfills [27]:

$$q_a = G_T \lambda e^{-\lambda t} \tag{2}$$

where  $G_T$  is the potential gas generation capacity ( $\text{kg}\cdot\text{m}^{-3}$ );  $\lambda$  is the degradation rate constant ( $\text{s}^{-1}$ ).

To account for the different gas generation rates at different depths in a layer with a linearly depositing rate, Equation (2) can be replaced as follows [23]:

$$q_a = G_T \lambda e^{-\lambda(t + \frac{h-z}{h} t_f)} \tag{3}$$

where  $t$  is the time elapsed since the emplacement of the layer (s);  $t_f$  is the time it took to fill the layer (s);  $h$  is the thickness of the layer (m).

The gas mass in the unit cell can be expressed as follows:

$$M_a = \rho_a V_a = \rho_a V_0 n (1 - S_l) \tag{4}$$

where  $V_a$  is the volume of gas in the unit cell ( $\text{m}^3$ );  $n$  is the porosity of the unit cell;  $S_l$  is the degree of liquid saturation.

Landfill gas is considered an ideal gas in MSW landfills. Therefore,

$$\rho_a = \frac{\bar{u}_a \omega}{RT} \tag{5}$$

where  $\omega$  is the average molecular weight of the gas ( $\text{kg}\cdot\text{mol}^{-1}$ );  $R$  is the universal gas constant ( $\text{J}\cdot\text{mol}^{-1}\cdot\text{K}^{-1}$ );  $T$  is the temperature in Kelvin of the gas (K);  $\bar{u}_a$  is the absolute gas pressure (Pa), which is expressed as

$$\bar{u}_a = u_a + u_{atm} \tag{6}$$

where  $u_a$  is the excess gas pressure (Pa);  $u_{atm}$  is the atmospheric pressure (101.3 kPa).

Based on Darcy’s law, the vertical flow velocity of the gas can be written as

$$v_z = -\frac{k_z}{\rho_a g} \frac{\partial u_a}{\partial z} \tag{7}$$

where  $k_z$  is the vertical gas permeability coefficient ( $\text{m}\cdot\text{s}^{-1}$ );  $g$  is the gravitational acceleration ( $\text{m}\cdot\text{s}^{-2}$ ).

Substituting Equations (4)–(7) into Equation (1) yields

$$\frac{1}{V_0} \frac{\partial V_a}{\partial t} = \frac{RTk_z}{\bar{u}_a \omega g} \frac{\partial^2 u_a}{\partial z^2} - \frac{n(1 - S_l)}{\bar{u}_a} \frac{\partial u_a}{\partial t} + \frac{RT}{\bar{u}_a \omega} q_a \tag{8}$$

According to Boyle’s law,

$$V_0 n(1 - S_l) \bar{u}_a = V_0 n_0(1 - S_{l0}) \bar{u}_0 \tag{9}$$

where  $\bar{u}_0$  is the initial absolute gas pressure (Pa);  $n_0$  is the initial porosity of the unit cell;  $S_{l0}$  is the initial degree of liquid saturation.

The variation of the excess gas pressure in a landfill with respect to  $u_{atm}$  can normally be neglected;  $\bar{u}_a$  is assumed to be constant. Therefore,

$$n(1 - S_l) = n_0(1 - S_{l0}) \tag{10}$$

The change rate of the gas volume in a unit volume of MSW can be obtained on the basis of the unsaturated soil gas phase constitutive equation [28], that is

$$\frac{1}{V_0} \frac{\partial V_a}{\partial t} = m_3^a \frac{\partial u_a}{\partial t} \tag{11}$$

where

$$m_3^a = m_2^a - m_1^a \tag{12}$$

In Equation (12),  $m_1^a$  is the coefficient of the change in gas volume corresponding to the main stress in the lateral confined condition ( $\text{Pa}^{-1}$ );  $m_2^a$  is the coefficient of the change in gas volume corresponding to the suction in the lateral confined condition ( $\text{Pa}^{-1}$ ).

Incorporating Equation (11) into Equation (8) gives

$$\frac{\partial u_a}{\partial t} = \alpha \frac{k_z}{g} \frac{\partial^2 u_a}{\partial z^2} + \alpha q_a \tag{13}$$

where

$$\alpha = -\frac{RT}{\omega [m_3^a \bar{u}_0 - n_0(1 - S_{l0})]} \tag{14}$$

A landfill consisting of a finite multilayer is shown in Figure 1.  $z_i$  and  $z_{i-1}$  are the upper depth and lower depth of the  $i$ th layer;  $z_m$  is the upper depth of the entire landfill.

According to Equations (13) and (14), the governing equation of a vertical gas flow in the  $i$ th layer is

$$\frac{\partial u_{a,i}}{\partial t} = \alpha_i \frac{k_{z,i}}{g} \frac{\partial^2 u_{a,i}}{\partial z^2} + \alpha_i q_{a,i}, \quad z_{i-1} \leq z \leq z_i, \quad i = 1, 2, \dots, m \tag{15}$$

where

$$\alpha_i = -\frac{RT_i}{\omega [m_{3,i}^a \bar{u}_{0,i} - n_{0,i}(1 - S_{l0,i})]} \tag{16}$$

where  $u_{a,i}$  is the excess gas pressure in the  $i$ th layer (Pa);  $k_{z,i}$  is the vertical gas permeability coefficient of the  $i$ th layer ( $\text{m}\cdot\text{s}^{-1}$ );  $q_{a,i}$  is the gas generation in  $i$ th layer ( $\text{kg}\cdot\text{m}^{-3}\cdot\text{s}^{-1}$ );  $T_i$  is the temperature in Kelvin of the  $i$ th layer (K);  $m_{3,i}^a = m_{2,i}^a - m_{1,i}^a$ ;  $m_{1,i}^a$  is the gas volume variation coefficient due to the net normal stress under the lateral confined condition in the

$i$ th layer ( $\text{Pa}^{-1}$ );  $m_{2,i}^a$  is the gas volume variation coefficient due to matric suction under the lateral confined condition in the  $i$ th layer ( $\text{Pa}^{-1}$ );  $n_{0,i}$  is the initial porosity of the  $i$ th layer;  $S_{l0,i}$  is the degree of liquid saturation in the  $i$ th layer;  $\bar{u}_{0,i}$  is the initial absolute gas pressure in the  $i$ th layer (Pa).

The boundary conditions are dependent on the operating scenarios of the landfills. The following operating scenarios were considered.

When a low-permeable cover is applied at the top surface of landfill, the boundary condition on the top surface of the landfill is [19]

$$\left. \frac{\partial u_{a,m}}{\partial z} \right|_{z=z_m} = \frac{R_t}{z_m} u_{a,m} \Big|_{z=z_m} \tag{17}$$

where  $R_t$  is the dimensionless property, as follows

$$R_t = \frac{k_{z,c} z_m}{k_{z,m} h_c} \tag{18}$$

In Equation (18),  $h_c$  is thickness of the cover (m);  $k_{z,c}$  is the vertical gas permeability coefficient for the top surface ( $\text{m}\cdot\text{s}^{-1}$ ).  $R_t$  is dimensionless and reflects the drainage efficiency at the top surface of the gas. The larger the value of  $R_t$ , the greater the drainage efficiency, that is, the smaller the hindrance effect on the top surface. When  $R_t$  is equal to zero, the boundary is absolutely impermeable to the gas, while when the  $R_t$  approaches infinity, the boundary is fully permeable to the gas.

If a fixed gas flux is specified at the bottom, the boundary condition on the bottom surface of the landfill is [8]

$$\frac{k_{z,1}}{g} \left. \frac{\partial u_{a,1}}{\partial z} \right|_{z=0} = J_l \tag{19}$$

where  $J_l$  is the gas flux rate applied at the base ( $\text{kg}\cdot\text{m}^{-2}\cdot\text{s}^{-1}$ ). When the bottom surface is absolutely impermeable to the gas,  $J_l = 0$ .

The continuity conditions of the adjacent two layers are

$$u_{a,i} \Big|_{z=z_i} = u_{a,i+1} \Big|_{z=z_i}, \quad k_{z,i} \left. \frac{\partial u_{a,i}}{\partial z} \right|_{z=z_i} = k_{z,i+1} \left. \frac{\partial u_{a,i+1}}{\partial z} \right|_{z=z_i}, \quad i = 1, 2, \dots, m - 1 \tag{20}$$

In the transient model, the initial conditions can be expressed as

$$u_{a,i} \Big|_{t=0} = u_{0,i}, \quad i = 1, 2, \dots, m \tag{21}$$

where  $u_{0,i}$  is the initial excess gas pressure in the  $i$ th layer (Pa).

### 3. Transient Analytical Solution and Application

#### 3.1. Transient Analytical Solution

The superposition method and orthogonal expansion technique were used to obtain the analytical solution of the transient model (see Appendix A). The solution of the excess gas pressure in the  $i$ th layer is expressed as

$$u_i(z, t) = a_i z + b_i + \sum_{j=1}^{\infty} [c_{i,j} \sin(\beta_{i,j} z) + d_{i,j} \cos(\beta_{i,j} z)] \left[ \int_0^t e^{-\alpha_i \frac{k_{z,i}}{g} \beta_{i,j}^2 (t-\tau)} T_{q,j}(\tau) d\tau + \varphi_j e^{-\alpha_i \frac{k_{z,i}}{g} \beta_{i,j}^2 t} \right] \tag{22}$$

where

$$a_1 = \frac{J_l g}{k_{z,1}}, \quad b_1 = \left( \frac{k_{z,1} h_m}{R_l k_{z,m}} - \frac{k_{z,1} z_m}{k_{z,m}} \right) a_1 - \sum_{q=1}^i \left( \frac{k_{z,1}}{k_{z,q}} - \frac{k_{z,1}}{k_{z,q+1}} \right) z_q a_1 \tag{23}$$

$$a_{i+1} = \frac{k_{z,1}}{k_{z,i+1}} a_1, \quad b_{i+1} = b_1 + \sum_{q=1}^i \left( \frac{k_{z,1}}{k_{z,q}} - \frac{k_{z,1}}{k_{z,q+1}} \right) z_q a_1, \quad i = 1, 2, \dots, m - 1$$

$$c_{1,j} = 0, d_{1,j} = 1 \tag{24}$$

The recursive relationship between  $c_{i,j}, d_{i,j}$  and  $c_{i+1,j}, d_{i+1,j}$  ( $i = 1, 2, \dots, m-1$ ) are

$$\begin{bmatrix} c_{i+1,j} \\ d_{i+1,j} \end{bmatrix} = \begin{bmatrix} F_{i,j}F_{i+1,j} + \chi_{i,j}F_{i,j}G_{i+1,j} & G_{i,j}F_{i+1,j} - \chi_{i,j}F_{i,j}G_{i+1,j} \\ F_{i,j}G_{i+1,j} - \chi_{i,j}F_{i,j}F_{i+1,j} & G_{i,j}G_{i+1,j} + \chi_{i,j}F_{i+1,j}G_{i+1,j} \end{bmatrix} \begin{bmatrix} c_{i,j} \\ d_{i,j} \end{bmatrix} \tag{25}$$

where

$$\chi_{i,j} = \frac{k_{z,i}\beta_{i,j}}{k_{z,i+1}\beta_{i+1,j}}, F_{i,j} = \sin(\beta_{i,j}z_i), G_{i,j} = \cos(\beta_{i,j}z_i) \tag{26}$$

$$\beta_{i,j} = \sqrt{\frac{\alpha_m k_{z,m}}{\alpha_i k_{z,i}}} \beta_{m,j} \tag{27}$$

$\beta_{m,j}$  indicates the roots of the following transcendental equation

$$S_{m-1,j} \begin{bmatrix} 0 \\ 1 \end{bmatrix} \begin{bmatrix} R_t \sin(\beta_{m,j}z_m) - z_m \cos(\beta_{m,j}z_m) \\ R_t \sin(\beta_{m,j}z_m) + z_m \cos(\beta_{m,j}z_m) \end{bmatrix}^T = 0 \tag{28}$$

where

$$S_{m-1,j} = \prod_{i=1}^{m-1} \begin{bmatrix} F_{i,j}F_{i+1,j} + \chi_{i,j}F_{i,j}G_{i+1,j} & G_{i,j}F_{i+1,j} - \chi_{i,j}F_{i,j}G_{i+1,j} \\ F_{i,j}G_{i+1,j} - \chi_{i,j}F_{i,j}F_{i+1,j} & G_{i,j}G_{i+1,j} + \chi_{i,j}F_{i+1,j}G_{i+1,j} \end{bmatrix} \tag{29}$$

In Equation (22),

$$T_{q,j}(t) = \left(\frac{1}{\psi}\right) \sum_{i=1}^m \int_{z_{i-1}}^{z_i} [c_{i,j} \sin(\beta_{i,j}z) + d_{i,j} \cos(\beta_{i,j}z)] \alpha_i q_{a,i} \left(\frac{1}{\alpha_i}\right) dz \tag{30}$$

$$\varphi_j = \left(\frac{1}{\psi}\right) \sum_{i=1}^m \int_{z_{i-1}}^{z_i} [c_{i,j} \sin(\beta_{i,j}z) + d_{i,j} \cos(\beta_{i,j}z)] (u_{0,i} - a_i z - b_i) \left(\frac{1}{\alpha_i}\right) dz \tag{31}$$

where

$$\psi = \sum_{i=1}^m \int_{z_{i-1}}^{z_i} [c_{i,j} \sin(\beta_{i,j}z) + d_{i,j} \cos(\beta_{i,j}z)]^2 \left(\frac{1}{\alpha_i}\right) dz \tag{32}$$

### 3.2. Verification of the Transient Analytical Solution

Yu et al. [19] proposed a vertical gas flow model for a landfill with layered MSW. The excess gas pressure of a landfill with two-layered MSWs was calculated by the semi-analytical solution in Yu et al.'s study. The calculation example of the two-layered landfill was adopted here. A schematic diagram of the landfill is shown in Figure 2a. The initial excess gas pressure was assumed to be 0. The parameter  $m_3^a$  in this study was approximately set to  $-1/E_0$  in  $m_k^a$  of Yu et al.'s study. The other parameters were the same as those in Yu et al.'s study. The values of the parameters are listed in Table 1. COMSOL Multiphysics is a widely used software based on the finite element method [29]. COMSOL simulation was used to verify the proposed transient analytical solution. The gas pressure at the bottom of the landfill obtained by the proposed transient analytical method and COMSOL is shown in Figure 2b. The relative error between the two methods was less than 0.5%. The analytical solution agreed with the numerical solution very well. Therefore, the correctness of the transient analytical solution was proved.

The proposed transient analytical method and Yu et al.'s semi-analytical method were compared. The gas pressure at the bottom of the landfill determined by the two methods is presented in Figure 2b. The results obtained by these two methods were in good agreement. However, the mechanical compression of the solid skeleton was coupled with gas pressure using the K-H viscoelastic model in Yu et al.'s study, while the unsaturated soils theory of Fredlund and Rahardjo [28] was adopted in this study. Thus, the parameter  $\alpha$  was

different in the two studies, which resulted in a slight difference in the gas pressure at the early times.

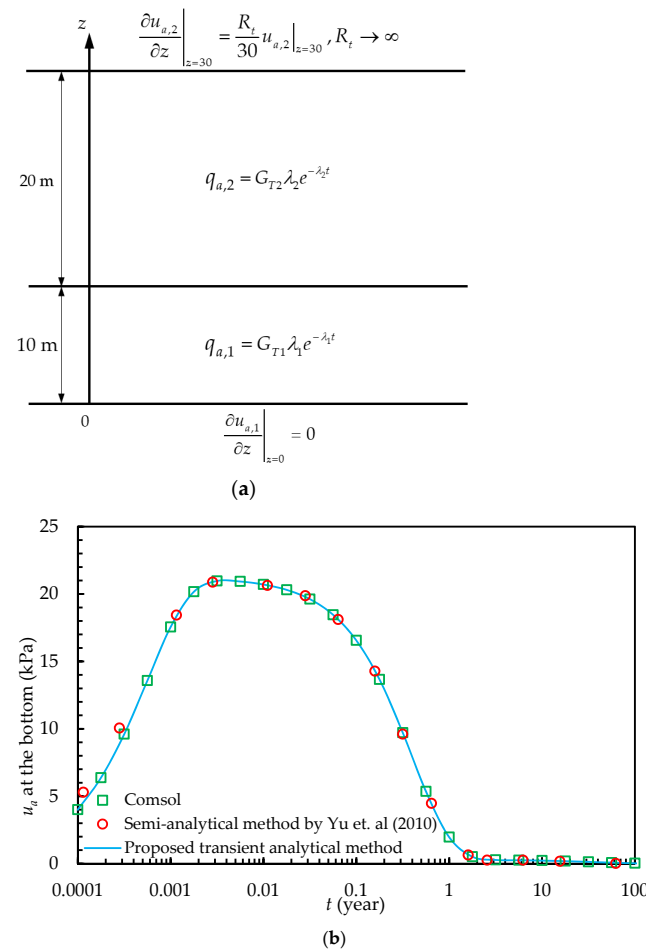


**Figure 2.** Comparison between the proposed transient analytical method and the numerical and semi-analytical method [19]. (a) Illustration of a two-layered landfill. (b) Comparison of the gas pressure values obtained using the different methods.

**Table 1.** Model parameters used by Yu et al. [19].

Parameters	Value
$k_{z,1}$ (m·s <sup>-1</sup> )	$5 \times 10^{-7}$
$k_{z,2}$ (m·s <sup>-1</sup> )	$1.2 \times 10^{-6}$
$n_{0,1}$	0.5
$n_{0,2}$	0.5
$S_{10,1}$	0
$S_{10,2}$	0
$u_{0,1}$ (Pa)	0
$u_{0,2}$ (Pa)	0
$T_1$ (K)	310
$T_2$ (K)	310
$m_{3,1}^a$ (kPa <sup>-1</sup> )	$-5 \times 10^{-20}$
$m_{3,2}^a$ (kPa <sup>-1</sup> )	$-2 \times 10^{-4}$
$\omega$ (kg·mol <sup>-1</sup> )	0.03
$R$ (J·mol <sup>-1</sup> ·K <sup>-1</sup> )	8.314
$G_{T1}$ (kg·m <sup>-3</sup> )	100
$G_{T2}$ (kg·m <sup>-3</sup> )	220
$\lambda_1$ (year <sup>-1</sup> )	2.523
$\lambda_2$ (year <sup>-1</sup> )	0.02523

### 3.3. Application of the Transient Analytical Solution

The effect of the parameter  $\alpha$  on the gas pressure was also investigated by the transient analytical solution. Three groups of the parameters  $S_{10,1}, S_{10,2}, T_1, T_2, m_{3,1}^a$  and  $m_{3,2}^a$  are shown in Table 2 and resulted in different values of the parameters  $\alpha_1$  and  $\alpha_2$ . The values of other parameters were the same as those in Table 1. It can be seen in Figure 3 that the effects of the parameter  $\alpha$  are only relevant for the early response.

**Table 2.** Parameters groups.

Parameter	Group 1	Group 2	Group 3
$\alpha_1$ ( $\text{m}^2 \cdot \text{s}^{-1}$ )	177,365	147,858	217,613
$\alpha_2$ ( $\text{m}^2 \cdot \text{s}^{-1}$ )	177,365	147,858	217,613
$S_{10,1}$	0	0	0.2
$S_{10,2}$	0	0	0.2
$T_1$ (K)	310	310	330
$T_2$ (K)	310	310	330
$m_{3,1}^a$ ( $\text{kPa}^{-1}$ )	0	$-8 \times 10^{-4}$	$-2 \times 10^{-4}$
$m_{3,2}^a$ ( $\text{kPa}^{-1}$ )	0	$-8 \times 10^{-4}$	$-2 \times 10^{-4}$

On the other hand, Equation (15) can be rewritten as follows

$$\frac{1}{\alpha_i} \frac{\partial u_{a,i}}{\partial t} = \frac{k_{z,i}}{g} \frac{\partial^2 u_{a,i}}{\partial z^2} + q_{a,i}, \quad z_{i-1} \leq z \leq z_i, \quad i = 1, 2, \dots, m \tag{33}$$

It can be seen from Table 2 that the values of the parameter  $\alpha_i$  were much larger than 1. Thus, the left side of Equation (15) approximated 0. This means that the time scale of the gas flow dynamics within the landfill could be neglected, and the gas flow could be approximated to a quasi-steady-state process, as follows

$$\frac{k_{z,i}}{g} \frac{\partial^2 u_{a,i}}{\partial z^2} + q_{a,i} = 0, \quad z_{i-1} \leq z \leq z_i, \quad i = 1, 2, \dots, m \tag{34}$$

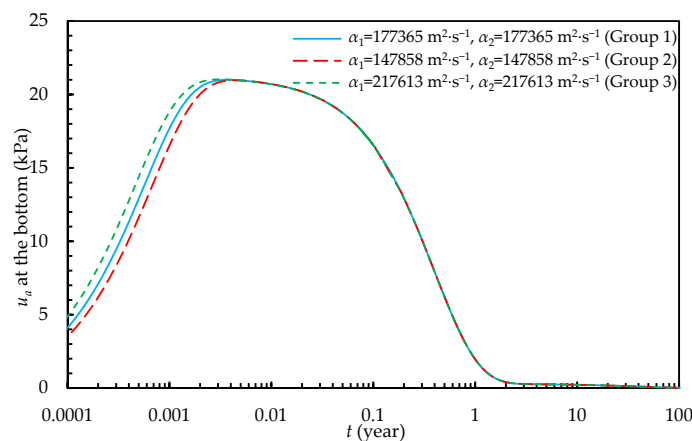


**Figure 3.** Effect of the parameter  $\alpha$  on the gas pressure.

## 4. Quasi-Steady-State Analytical Solution and Validation

### 4.1. Quasi-Steady-State Analytical Solution

Solving the ordinary differential Equation (34) by the direct integration method, the quasi-steady-state analytical solution can be obtained as follows

$$u_{a,i}(z, t) = -\frac{g}{k_{z,i}} Q_{2,i} + r_i z + s_i, \quad z_{i-1} \leq z \leq z_i, \quad i = 1, 2, \dots, m \tag{35}$$

where

$$Q_{2,i} = \int Q_{1,i} dz, \quad Q_{1,i} = \int q_{a,i} dz \tag{36}$$

Substituting Equation (35) into the boundary conditions of Equations (17) and (19) yields

$$-\frac{g}{k_{z,m}} Q_{1,m}|_{z=z_m} + r_m = \frac{R_t}{z_m} \left[ -\frac{g}{k_{z,m}} Q_{2,m}|_{z=z_m} + r_m z_m + s_m \right] \tag{37}$$

$$-\frac{g}{k_{z,1}} Q_{1,1}|_{z=0} + r_1 = \frac{J_l g}{k_{z,1}} \tag{38}$$

Substituting Equation (35) into the continuity conditions Equation (20) yields

$$-\frac{g}{k_{z,i}} Q_{2,i}|_{z=z_i} + r_i z_i + s_i = -\frac{g}{k_{z,i}} Q_{2,i+1}|_{z=z_i} + r_{i+1} z_i + s_{i+1} \tag{39}$$

$$-g Q_{1,i}|_{z=z_i} + k_{z,i} r_i = -g Q_{1,i+1}|_{z=z_i} + k_{z,i+1} r_{i+1} \tag{40}$$

Using Equations (37)–(40),  $r_i$  and  $s_i$  can be determined in the form of matrices, as follows

$$\mathbf{C} = \mathbf{D}^{-1} \mathbf{E} \tag{41}$$

where  $C, D, E$  are a  $2n \times 1, 2n \times 2n, 2n \times 1$  matrix, as follows

$$\mathbf{C} = [r_m \quad s_m \quad \dots \quad r_i \quad s_i \quad \dots \quad r_1 \quad s_1]^T \tag{42}$$

$$\mathbf{D} = \begin{bmatrix} \mathbf{D}_{up} & \dots & 0 & \dots & 0 \\ \mathbf{D}_{n-1} & \dots & 0 & \dots & 0 \\ \dots & \dots & \dots & \dots & \dots \\ 0 & \dots & \mathbf{D}_i & \dots & 0 \\ \dots & \dots & \dots & \dots & \dots \\ 0 & \dots & 0 & \dots & \mathbf{D}_1 \\ 0 & \dots & 0 & \dots & \mathbf{D}_{lo} \end{bmatrix} \tag{43}$$

$$\mathbf{E} = [\mathbf{E}_{up} \quad \mathbf{E}_{n-1} \quad \dots \quad \mathbf{E}_i \quad \dots \quad \mathbf{E}_1 \quad \mathbf{E}_{lo}]^T \tag{44}$$

In Equations (43) and (44),  $\mathbf{0}$  indicates a zero matrix,

$$\mathbf{D}_i = \begin{bmatrix} z_i & 1 & -z_i & -1 \\ k_{z,i} & 0 & -k_{z,i+1} & 0 \end{bmatrix} \tag{45}$$

$$\mathbf{D}_{up} = \left[ 1 - \frac{R_t}{z_m} z_m \quad -\frac{R_t}{z_m} \quad 0 \quad 0 \right] \tag{46}$$

$$\mathbf{D}_{lo} = [0 \quad 0 \quad 1 \quad 0] \tag{47}$$

$$\mathbf{E}_i = \left[ \frac{g}{k_{z,i}} Q_{2,i}|_{z=z_i} - \frac{g}{k_{z,i+1}} Q_{2,i+1}|_{z=z_i} \quad g Q_{1,i}|_{z=z_i} - g Q_{1,i+1}|_{z=z_i} \right] \tag{48}$$

$$\mathbf{E}_{up} = \left[ -\frac{g}{k_{z,m}} \frac{R_t}{h_m} Q_{2,m}|_{z=z_m} + \frac{g}{k_{z,m}} Q_{1,m}|_{z=z_m} \right] \tag{49}$$

$$\mathbf{E}_{lo} = \left[ \frac{J_l g}{k_{z,1}} + \frac{g}{k_{z,1}} Q_{1,1}|_{z=0} \right] \tag{50}$$

#### 4.2. Comparison of the Quasi-Steady-State and Transient Solutions

A new calculation example was proposed, in which the temporal and spatial variability of the gas generation rate was considered. A landfill containing two layers of MSW and an intermediate cover was considered. The landfill is illustrated in Figure 4. The height of each MSW layer was assumed to be 10 m, and the filling of each MSW layer took 2 years. The filling time of the intermediate cover was much shorter than the time required to form

an MSW layer and was not considered in the study. A high mass fraction of food waste was shown to result in a high liquid saturation of wastes in China [30,31]. The values of porosity  $n$  and liquid saturation  $S_l$  were selected according to their common value range for landfills in China. The gas permeability of MSW corresponding to a specific porosity  $n$  and liquid saturation  $S_l$  was based on the experimental result by Shi et al. [32]. Two kinds of boundary conditions on the top surface of the landfill were considered, i.e., with or without the top cover. When there is no top cover,  $R_t$  approaches infinity. The thickness and vertical gas permeability of the top cover are shown in Table 3. The initial excess gas pressure was assumed to be 0 in the following analysis.

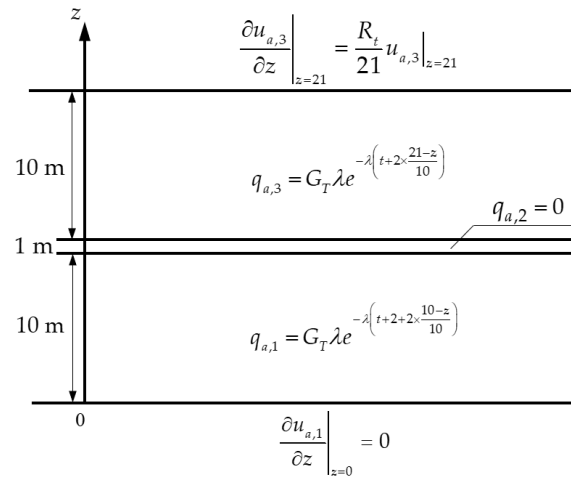


Figure 4. Illustration of a landfill containing two layers of MSW and an intermediate cover.

Equation (3) was adopted to describe the gas generation in the two MSW layers. The gas generation in the first MSW layer was as follows

$$q_{a,1} = G_T \lambda e^{-\lambda \left( t + 2 + 2 \times \frac{10-z}{10} \right)} \tag{51}$$

The gas generation in the second MSW layer was as follows

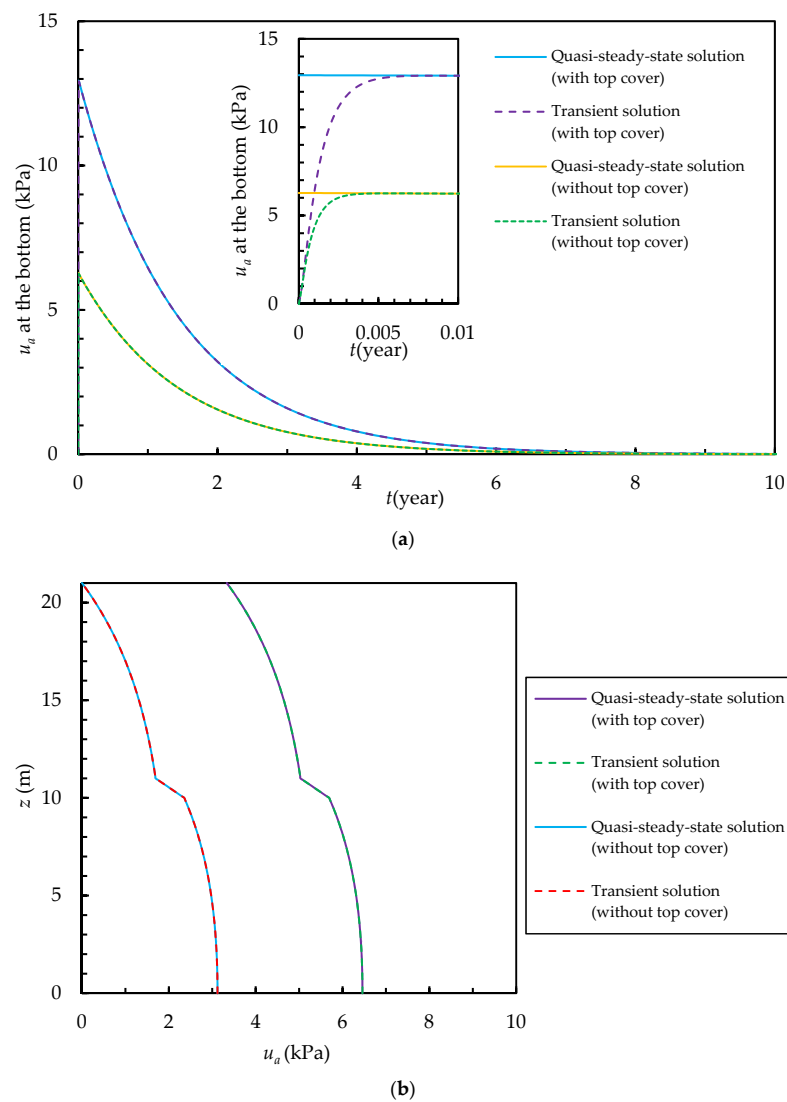
$$q_{a,3} = G_T \lambda e^{-\lambda \left( t + 2 + 2 \times \frac{21-z}{10} \right)} \tag{52}$$

Table 3. Model parameters.

Parameters	Value
$k_{z,1}$ ( $\text{m} \cdot \text{s}^{-1}$ ) [32]	$1 \times 10^{-7}$
$k_{z,2}$ ( $\text{m} \cdot \text{s}^{-1}$ ) [21]	$6 \times 10^{-8}$
$k_{z,3}$ ( $\text{m} \cdot \text{s}^{-1}$ ) [32]	$3 \times 10^{-7}$
$k_c$ ( $\text{m} \cdot \text{s}^{-1}$ ) [19]	$3 \times 10^{-8}$
$h_c$ (m) [19]	1
$n_{0,1}$ [30,31]	0.667
$n_{0,2}$ [31,32]	0.333
$n_{0,3}$ [30,31]	0.737
$S_{l0,1}$ [30,31]	0.8
$S_{l0,2}$ [30,31]	0.78
$S_{l0,3}$ [30,31]	0.75
$T_1$ (K) [19]	310
$T_2$ (K) [19]	310
$T_3$ (K) [19]	310
$m_{3,1}^a$ ( $\text{kPa}^{-1}$ ) [28]	$-6 \times 10^{-4}$
$m_{3,2}^a$ ( $\text{kPa}^{-1}$ ) [28]	$-6 \times 10^{-4}$
$m_{3,3}^a$ ( $\text{kPa}^{-1}$ ) [28]	$-6 \times 10^{-4}$
$\omega$ ( $\text{kg} \cdot \text{mol}^{-1}$ ) [8,23]	0.03
$R$ ( $\text{J} \cdot \text{mol}^{-1} \cdot \text{K}^{-1}$ ) [8,23]	8.314
$G_T$ ( $\text{kg} \cdot \text{m}^{-3}$ ) [21]	138
$\lambda$ ( $\text{year}^{-1}$ ) [21]	0.7

All parameters are listed in Table 3. They were within the typical ranges suggested from previous publications.

The evolution of gas pressure with time at the bottom of the landfill was calculated by the transient analytical solution and quasi-steady-state analytical solution, as shown in Figure 5a. The evolution of the gas pressure with depth at  $t = 1$  year was also calculated by the transient analytical solution and quasi-steady-state analytical solution, as shown in Figure 5b. The relative error of the gas pressures ( $t > 0.006$  year) determined using the two methods was less than 0.5%. The results obtained from the transient analytical solution and quasi-steady-state analytical solution were in good agreement. There was only a slight difference in the gas pressure at an early time ( $<0.006$  year). This demonstrates that the quasi-steady-state solution can reliably estimate the gas pressure in landfills.



**Figure 5.** Gas pressure calculated by the transient analytical solution and the quasi-steady-state analytical solution. (a) Gas pressure changing with time. (b) Gas pressure changing with depth at  $t = 1$  year.

#### 4.3. Comparison of the Quasi-Steady-State and Steady-State Solutions

When the gas generation rate  $q_{a,i}$  in Equation (34) is a constant, the quasi-steady-state governing equations become the steady-state governing equations. Li et al. [9] proposed a steady-state analytical model for the vertical gas flow in a landfill with layered MSW. The values of the gas generation rate in each layer at a certain time used in the steady-state

model are the average values of the gas generation rate in the layer or the gas generation rate corresponding to the average age of each layer.

The average value of gas generation  $\bar{q}_{a,i}$  was calculated as follows

$$\bar{q}_{a,i} = \frac{1}{z_i - z_{i-1}} \int_{z_{i-1}}^{z_i} q_{a,i} dz \tag{53}$$

The landfill in Section 4.2 was considered. The gas pressure was calculated by the proposed quasi-steady-state solution and the steady-state solution by Li et al. [9]. As shown in Figure 6, the steady-state model resulted in an error in the estimation of gas pressure. For instance, the gas pressure at the bottom of the landfill without a top cover obtained by the steady-state solution using the average gas generation rate corresponding to the average age was 8.7% greater than that obtained by the quasi-steady-state solution, at  $t = 0.5$  year. The gas pressure at the bottom of the landfill with a top cover obtained by the steady-state solution using the average gas generation rate was 8% greater than that obtained by the quasi-steady-state solution, at  $t = 1$  year. Thus, it is necessary to consider the variation of the gas generation rate in the depth of a landfill in relation to the fill age when predicting the gas pressure in MSW landfills.

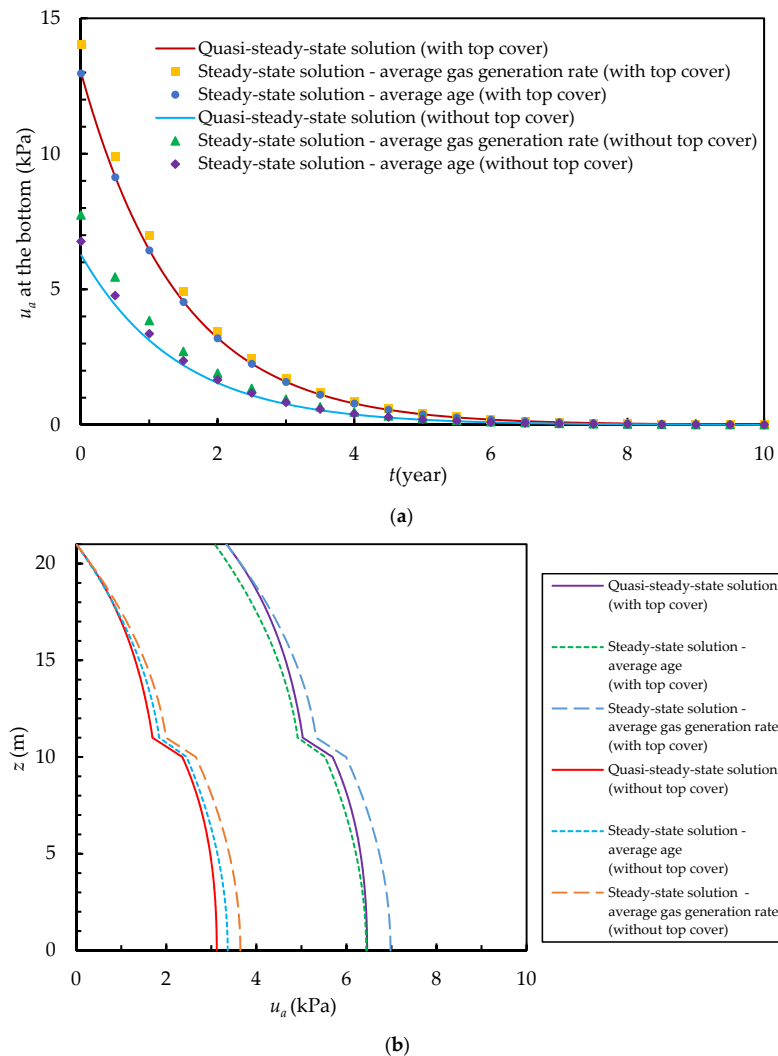


**Figure 6.** Changes of the gas pressure with time, calculated by the quasi-steady-state analytical solution and the steady-state analytical solution. (a) Gas pressure changing with time. (b) Gas pressure changing with depth at  $t = 1$  year.

### 5. Conclusions

In this paper, a one-dimensional analytical model was proposed to simulate the vertical gas flow in a landfill with layered MSW. Temporal and spatial variations of the gas generation rate in the MSW were considered. A transient analytical solution was obtained by the superposition method and the orthogonal expansion technique. A quasi-steady-state analytical solution was also obtained by the direct integration method. Several conclusions can be drawn on the basis of the adopted solution, as shown below:

- (1) According to the results of the parameter analysis by the transient analytical solution, the vertical gas flow in landfills can be simplified to a quasi-steady-state flow.
- (2) The gas pressure values obtained by the transient and quasi-steady-state analytical solutions were in good agreement. There was only a slight difference in the gas pressure at the early times. The quasi-steady-state solution can reliably estimate the gas pressure in landfills.
- (3) Using the average gas generation rate or the gas generation rate corresponding to the average age of the MSW layer in the steady-state model resulted in an error in the estimation of gas pressure in landfills.
- (4) The axisymmetric transient and quasi-steady-state analytical models for the gas flow around a vertical well in a layered landfill can be proposed by extension of the results of this paper.

**Author Contributions:** Conceptualization, X.W. and J.S.; methodology, X.W.; software, X.W.; validation, T.Z.; formal analysis, Y.L.; investigation, S.S.; resources, Y.L.; data curation, S.S.; writing—original draft preparation, X.W.; writing—review and editing, X.W. and J.S.; visualization, T.Z.; supervision, J.S.; project administration, Y.L.; funding acquisition, S.S. All authors have read and agreed to the published version of the manuscript.

**Funding:** This research was funded by the National Natural Science Foundation of China, grant number 42002288, 41877222, 42002286, 42007253.

**Data Availability Statement:** Not applicable.

**Acknowledgments:** The financial support from the National Natural Science Foundation of China is gratefully acknowledged. The authors would like to thank the editor and reviewers in advance for carefully dealing with this manuscript.

**Conflicts of Interest:** The authors declare no conflict of interest.

### Appendix A. Development of the Transient Analytical Solution

Both the governing Equation (15) and the boundary condition Equation (19) are non-homogeneous. To transform the nonhomogeneous boundary conditions into homogeneous boundary conditions, a new function  $v_i$  was introduced.

$v_i$  satisfies the homogeneous governing equation and nonhomogeneous boundary condition as follows

$$\frac{\partial v_i}{\partial t} = 0, \quad z_{i-1} \leq z \leq z_i, \quad i = 1, 2, \dots, m \tag{A1}$$

$$\left. \frac{\partial v_m}{\partial z} \right|_{z=z_m} = \frac{R_t}{z_m} v_m \Big|_{z=z_m} \tag{A2}$$

$$\left. \frac{k_{z,1}}{g} \frac{\partial v_1}{\partial z} \right|_{z=0} = J_l \tag{A3}$$

The continuity conditions of  $v_i$  are

$$v_i \Big|_{z=z_i} = v_{i+1} \Big|_{z=z_i}, \quad k_{z,i} \left. \frac{\partial v_i}{\partial z} \right|_{z=z_i} = k_{z,i+1} \left. \frac{\partial v_{i+1}}{\partial z} \right|_{z=z_i}, \quad i = 1, 2, \dots, m - 1 \tag{A4}$$

$v_i$  can be obtained as follows

$$v_i = a_i z + b_i \tag{A5}$$

Substituting Equation (A5) into Equations (A2)–(A4),  $a_i$  and  $b_i$  can be determined as:

$$a_1 = \frac{J_1 g}{k_{z,1}}, b_1 = \left( \frac{k_{z,1} h_m}{R_t k_{z,m}} - \frac{k_{z,1} z_m}{k_{z,m}} \right) a_1 - \sum_{q=1}^i \left( \frac{k_{z,1}}{k_{z,q}} - \frac{k_{z,1}}{k_{z,q+1}} \right) z_q a_1$$

$$a_{i+1} = \frac{k_{z,1}}{k_{z,i+1}} a_1, b_{i+1} = b_1 + \sum_{q=1}^i \left( \frac{k_{z,1}}{k_{z,q}} - \frac{k_{z,1}}{k_{z,q+1}} \right) z_q a_1, i = 1, 2, \dots, m - 1$$
(A6)

The solution of  $u_{a,i}$  can be obtained as follows

$$u_{a,i} = v_i + w_i, z_{i-1} \leq z \leq z_i, i = 1, 2, \dots, m$$
(A7)

The substitution of Equations (A1) and (A7) into Equation (15) results in

$$\frac{\partial w_i}{\partial t} = \alpha_i \frac{k_{z,i}}{g} \frac{\partial^2 w_i}{\partial z^2} + \alpha_i q_{a,i}, z_{i-1} \leq z \leq z_i, i = 1, 2, \dots, m$$
(A8)

Using Equations (17), (19), (A2), (A3) and (A7), the boundary conditions of  $w_i$  are as follows

$$\left. \frac{\partial w_m}{\partial z} \right|_{z=z_m} = \frac{R_t}{z_m} w_m \Big|_{z=z_m}$$
(A9)

$$\left. \frac{\partial w_1}{\partial z} \right|_{z=0} = 0$$
(A10)

Using Equations (20), (A4) and (A7), the continuity conditions of  $w_i$  are

$$w_i \Big|_{z=z_i} = w_{i+1} \Big|_{z=z_i}, k_{z,i} \left. \frac{\partial w_i}{\partial z} \right|_{z=z_i} = k_{z,i+1} \left. \frac{\partial w_{i+1}}{\partial z} \right|_{z=z_i}, i = 1, 2, \dots, m - 1$$
(A11)

Using Equations (21), (A5) and (A7), the initial conditions of  $w_i$  are as follows

$$w_i \Big|_{t=0} = u_{0,i} - v_i, i = 1, 2, \dots, m$$
(A12)

The above nonhomogeneous linear partial differential Equation (A8) subject to the homogeneous boundary conditions can be solved using the method of eigenfunction expansion.

Let  $w_{h,i}(z,t)$  be the solution of the homogeneous differential Equation (A8), which is used to obtain the characteristic function. According to Equation (A8), the governing equation of  $w_{h,i}$  is

$$\frac{\partial w_{h,i}}{\partial t} = \alpha_i \frac{k_{z,i}}{g} \frac{\partial^2 w_{h,i}}{\partial z^2}, z_{i-1} \leq z \leq z_i, i = 1, 2, \dots, m$$
(A13)

According to Equations (A9) and (A10), the boundary conditions of  $w_{h,i}$  are as follows

$$\left. \frac{\partial w_{h,m}}{\partial z} \right|_{z=z_m} = \frac{R_t}{z_m} w_{h,m} \Big|_{z=z_m}$$
(A14)

$$\left. \frac{\partial w_{h,1}}{\partial z} \right|_{z=0} = 0$$
(A15)

Using Equations (20), (A4) and (A7), the continuity conditions of  $w_{h,i}$  are

$$w_{h,i} \Big|_{z=z_i} = w_{h,i+1} \Big|_{z=z_i}, k_{z,i} \left. \frac{\partial w_{h,i}}{\partial z} \right|_{z=z_i} = k_{z,i+1} \left. \frac{\partial w_{h,i+1}}{\partial z} \right|_{z=z_i}, i = 1, 2, \dots, m - 1$$
(A16)

$w_{h,i}$  can be expressed as follows

$$w_{h,i}(z,t) = Z_i(z) T_i(t)$$
(A17)

where  $Z_i(z)$  and  $T_i(t)$  are unknown functions to be determined.  
 Substituting Equation (A17) into Equation (A13) results in

$$\frac{1}{\alpha_i T_i(t)} \frac{dT_i(t)}{dt} = \frac{1}{Z_i(z)} \frac{d^2 Z_i(z)}{dz^2} = -\beta_i^2, \quad i = 1, 2, \dots, m \tag{A18}$$

where  $\beta_i$  is the separation constant.

Equation (A18) can be rewritten as follows

$$\frac{d^2 Z_i(z)}{dz^2} + \beta_i^2 Z_i(z) = 0, \quad \frac{dT_i(t)}{dt} + \alpha_i \beta_i^2 T_i(t) = 0, \quad i = 1, 2, \dots, m \tag{A19}$$

According to the solutions for  $Z_i(z)$  and  $T_i(t)$  in Equation (A19),  $w_{h,i}$  can be expressed as follows

$$w_{h,i}(z, t) = \sum_{j=1}^{\infty} Z_{i,j}(z) T_{i,j}(t) \tag{A20}$$

where

$$Z_{i,j}(z) = c_{i,j} \sin(\beta_{i,j}z) + d_{i,j} \cos(\beta_{i,j}z) \tag{A21}$$

$$T_{i,j}(t) = e^{-\alpha_{i,j} \beta_{i,j}^2 t} \tag{A22}$$

Substituting Equations (A20)–(A22) into Equation (A15) yields

$$c_{1,j} = 0 \tag{A23}$$

Without loss of generality,  $d_{1,j}$  is assumed to be 1.

Substituting Equations (A20)–(A22) into Equation (A16) yields

$$\beta_{i,j} = \sqrt{\frac{\alpha_m k_{z,m}}{\alpha_i k_{z,i}}} \beta_{m,j} \tag{A24}$$

$$c_{i,j} \sin(\lambda_{i,j} z_{i,j}) + d_{i,j} \cos(\lambda_{i,j} z_{i,j}) = c_{i+1,j} \sin(\lambda_{i+1,j} z_{i,j}) + d_{i+1,j} \cos(\lambda_{i+1,j} z_{i,j}) \tag{A25}$$

$$k_{z,i} \lambda_{i,j} [c_{i,j} \cos(\lambda_{i,j} z_i) - d_{i,j} \sin(\lambda_{i,j} z_i)] = k_{z,i+1} \lambda_{i+1,j} [c_{i+1,j} \cos(\lambda_{i+1,j} z_i) - d_{i+1,j} \sin(\lambda_{i+1,j} z_i)] \tag{A26}$$

From Equations (A25) and (A26), the recursive relationship between  $c_{i,j}$ ,  $d_{i,j}$  and  $c_{i+1,j}$ ,  $d_{i+1,j}$  ( $i = 1, 2, \dots, m - 1$ ) are obtained as follows

$$\begin{bmatrix} c_{i+1,j} \\ d_{i+1,j} \end{bmatrix} = \begin{bmatrix} F_{i,j} F_{i+1,j} + \chi_{i,j} F_{i,j} G_{i+1,j} & G_{i,j} F_{i+1,j} - \chi_{i,j} F_{i,j} G_{i+1,j} \\ F_{i,j} G_{i+1,j} - \chi_{i,j} F_{i,j} F_{i+1,j} & G_{i,j} G_{i+1,j} + \chi_{i,j} F_{i+1,j} G_{i+1,j} \end{bmatrix} \begin{bmatrix} c_{i,j} \\ d_{i,j} \end{bmatrix} \tag{A27}$$

In Equation (A27),

$$\chi_{i,j} = \frac{k_{z,i} \beta_{i,j}}{k_{z,i+1} \beta_{i+1,j}}, \quad F_{i,j} = \sin(\beta_{i,j} z_i), \quad G_{i,j} = \cos(\beta_{i,j} z_i) \tag{A28}$$

Substituting Equations (A20)–(A22) into Equation (A14), a transcendental equation of  $\beta_{m,j}$  is obtained as follows

$$\mathbf{S}_{m-1,j} \begin{bmatrix} 0 \\ 1 \end{bmatrix} \begin{bmatrix} R_t \sin(\beta_{m,j} z_m) - h_m \cos(\beta_{m,j} z_m) \\ R_t \sin(\beta_{m,j} z_m) + h_m \cos(\beta_{m,j} z_m) \end{bmatrix}^T = 0 \tag{A29}$$

In Equation (A29),

$$\mathbf{S}_{m-1,j} = \prod_{i=1}^{m-1} \begin{bmatrix} F_{i,j} F_{i+1,j} + \chi_{i,j} F_{i,j} G_{i+1,j} & G_{i,j} F_{i+1,j} - \chi_{i,j} F_{i,j} G_{i+1,j} \\ F_{i,j} G_{i+1,j} - \chi_{i,j} F_{i,j} F_{i+1,j} & G_{i,j} G_{i+1,j} + \chi_{i,j} F_{i+1,j} G_{i+1,j} \end{bmatrix} \tag{A30}$$

According to the Sturm–Liouville theory [33], the characteristic function Equation (A21) satisfies the following orthogonal relationship

$$\sum_{i=1}^m \int_{z_{i-1}}^{z_i} Z_{i,j}(z) Z_{i,p}(z) \left( \frac{1}{\alpha_i} \right) dz = \begin{cases} 0, & j \neq p \\ \psi, & j = p \end{cases} \quad (\text{A31})$$

Based on the orthogonal expansion technique and the characteristic function obtained above,  $w_i$  is expressed as

$$w_i(z, t) = \sum_{j=1}^{\infty} Z_{i,j}(z) T_{w,j}(t) \quad (\text{A32})$$

The orthogonal expansion of  $q_{w,i}$  can be expressed as follows

$$q_{w,i} = \sum_{j=1}^{\infty} Z_{i,j}(z) T_{q,j}(t) \quad (\text{A33})$$

where

$$T_{q,j}(t) = \left( \frac{1}{\psi} \right) \sum_{i=1}^m \int_{z_{i-1}}^{z_i} Z_{i,j}(z) \alpha_i q_{a,i} \left( \frac{1}{\alpha_i} \right) dz \quad (\text{A34})$$

Substituting Equations (A32) and (A33) into Equation (A8), an ordinary differential equation is obtained as follows

$$\frac{dT_{w,j}(t)}{dt} + \alpha_i \frac{k_{z,i}}{g} \beta_{i,j}^2 T_{w,j}(t) = T_{q,j}(t) \quad (\text{A35})$$

The solution of the ordinary differential Equation (A35) is obtained as:

$$T_{w,j}(t) = \int_0^t e^{-\alpha_i \frac{k_{z,i}}{g} \beta_{i,j}^2 (t-\tau)} T_{q,j}(\tau) d\tau + \varphi_j e^{-\alpha_i \frac{k_{z,i}}{g} \beta_{i,j}^2 t} \quad (\text{A36})$$

Substituting Equations (A32) and (A36) into Equation (A12),  $\varphi_j$  is calculated using the orthogonality of the characteristic function  $Z_{i,j}(z)$  as follows

$$\varphi_j = \left( \frac{1}{\psi} \right) \sum_{i=1}^m \int_{z_{i-1}}^{z_i} Z_{i,j}(z) w_i|_{t=0} \left( \frac{1}{\alpha_i} \right) dz \quad (\text{A37})$$

## References

1. Parameswaran, T.G.; Sivakumar Babu, G.L. Design of gas collection systems: Issues and challenges. *Waste Manag. Res.* **2022**, 0734242X221086949. [[CrossRef](#)] [[PubMed](#)]
2. Duan, Z.; Scheutz, C.; Kjeldsen, P. Trace gas emissions from municipal solid waste landfills: A review. *Waste Manag.* **2021**, *119*, 39–62. [[CrossRef](#)] [[PubMed](#)]
3. Paraskaki, I.; Lazaridis, M. Quantification of landfill emissions to air: A case study of the Ano Liosia landfill site in the greater Athens area. *Waste Manag. Res.* **2005**, *23*, 199–208. [[CrossRef](#)] [[PubMed](#)]
4. Tian, H.; Gao, J.; Hao, J.; Lu, L.; Zhu, C.; Qiu, P. Atmospheric pollution problems and control proposals associated with solid waste management in China: A review. *J. Hazard. Mater.* **2013**, *252*, 142–154. [[CrossRef](#)]
5. Liu, Y.; Lu, W.; Dastyar, W.; Liu, Y.; Guo, H.; Fu, X.; Li, H.; Meng, R.; Zhao, M.; Wang, H. Fugitive halocarbon emissions from working face of municipal solid waste landfills in China. *Waste Manag.* **2017**, *70*, 149–157. [[CrossRef](#)]
6. Ke, H.; Hu, J.; Chen, Y.M.; Lan, J.W.; Zhan, L.T.; Meng, M.; Yang, Y.Q.; Li, Y.C. Foam-induced high gas pressures in wet municipal solid waste landfills. *Géotechnique* **2021**, *72*, 860–871. [[CrossRef](#)]
7. Shu, S.; Li, Y.; Sun, Z.; Shi, J. Effect of gas pressure on municipal solid waste landfill slope stability. *Waste Manag. Res.* **2022**, *40*, 323–330. [[CrossRef](#)]
8. Townsend, T.G.; Wise, W.R.; Jain, P. One-dimensional gas flow model for horizontal gas collection systems at municipal solid waste landfills. *J. Environ. Eng.* **2005**, *131*, 1716–1723. [[CrossRef](#)]
9. Li, Y.C.; Zheng, J.; Chen, Y.M.; Guo, R.Y. One-dimensional transient analytical solution for gas pressure in municipal solid waste landfills. *J. Environ. Eng.* **2013**, *139*, 1441–1445. [[CrossRef](#)]
10. Zeng, G. Study on landfill gas migration in landfilled municipal solid waste based on gas-solid coupling model. *Environ. Prog. Sustain.* **2020**, *39*, e13352. [[CrossRef](#)]

11. Feng, S.J.; Wu, S.J.; Zheng, Q.T. Design method of a modified layered aerobic waste landfill divided by coarse material. *Environ. Sci. Pollut. Res.* **2021**, *28*, 2182–2197. [[CrossRef](#)] [[PubMed](#)]
12. Zhang, T.; Shi, J.; Qian, X.; Ai, Y. Temperature monitoring during a water-injection test using a vertical well in a newly filled MSW layer of a landfill. *Waste Manag. Res.* **2019**, *37*, 530–541. [[CrossRef](#)] [[PubMed](#)]
13. Jain, P.; Powell, J.; Townsend, T.G.; Reinhart, D.R. Air permeability of waste in a municipal solid waste landfill. *J. Environ. Eng.* **2012**, *131*, 1565–1573. [[CrossRef](#)]
14. Zhang, W.; Lin, M. Evaluating the dual porosity of landfilled municipal solid waste. *Environ. Sci. Pollut. Res.* **2019**, *26*, 12080–12088. [[CrossRef](#)] [[PubMed](#)]
15. Jung, Y.J.; Imhoff, P.T.; Augenstein, D.C.; Yazdani, R. Influence of high-permeability layers for enhancing landfill gas capture and reducing fugitive methane emissions from landfills. *J. Environ. Eng.* **2009**, *135*, 138–146. [[CrossRef](#)]
16. Hettiarachchi, C.H.; Meegoda, J.N.; Tavantzis, J.; Hettiaratchi, P. Numerical model to predict settlements coupled with landfill gas pressure in bioreactor landfills. *J. Hazard. Mater.* **2007**, *139*, 514–522. [[CrossRef](#)]
17. Zhang, T.; Shi, J.; Wu, X.; Lin, H.; Li, X. Simulation of gas transport in a landfill with layered new and old municipal solid waste. *Sci. Rep.* **2021**, *11*, 9436. [[CrossRef](#)]
18. Xie, H.; Fei, S.; He, H.; Zhang, A.; Ni, J.; Chen, Y. Field investigation and numerical modelling of gas extraction in a heterogeneous landfill with high leachate level. *Environ. Sci. Pollut. Res.* **2022**, 1–17. [[CrossRef](#)]
19. Yu, L.; Batlle, F.; Carrera, J.; Lloret, A. A coupled model for prediction of settlement and gas flow in MSW landfills. *Int. J. Numer. Anal. Meth. Geomech.* **2010**, *34*, 1169–1190. [[CrossRef](#)]
20. Li, Y.C.; Cleall, P.J.; Ma, X.F.; Zhan, T.L.; Chen, Y.M. Gas pressure model for layered municipal solid waste landfills. *J. Environ. Eng.* **2012**, *138*, 752–760. [[CrossRef](#)]
21. Feng, S.J.; Zheng, Q.T. A two-dimensional gas flow model for layered municipal solid waste landfills. *Comput. Geotech.* **2015**, *63*, 135–145. [[CrossRef](#)]
22. Feng, S.J.; Zheng, Q.T.; Xie, H.J. A gas flow model for layered landfills with vertical extraction wells. *Waste Manag.* **2017**, *66*, 103–113. [[CrossRef](#)] [[PubMed](#)]
23. Arigala, S.G.; Tsotsis, T.T.; Webster, I.A.; Yortsos, Y.C. Gas generation, transport, and extraction in landfills. *J. Environ. Eng.* **1995**, *121*, 33–44. [[CrossRef](#)]
24. Amini, H.R.; Reinhart, D.R.; Niskanen, A. Comparison of first-order-decay modeled and actual field measured municipal solid waste landfill methane data. *Waste Manag.* **2013**, *33*, 2720–2728. [[CrossRef](#)]
25. Majdinasab, A.; Zhang, Z.; Yuan, Q. Modelling of landfill gas generation: A review. *Rev. Environ. Sci. Bio/Technol.* **2017**, *16*, 361–380. [[CrossRef](#)]
26. Liu, X.D.; Shi, J.; Qian, X.; Hu, Y.; Peng, G. One-dimensional model for municipal solid waste (MSW) settlement considering coupled mechanical-hydraulic-gaseous effect and concise calculation. *Waste Manag.* **2011**, *31*, 2473–2483. [[CrossRef](#)]
27. SWAMA. *Comparison of Models for Predicting Landfill Methane Recovery Publication*; The Solid Waste Association of North America (SWANA): San Diego, CA, USA, 1998.
28. Fredlund, D.G.; Rahardjo, H. *Soil Mechanics for Unsaturated Soils*; John Wiley & Sons: Hoboken, NJ, USA, 1993.
29. COMSOL. COMSOL Multiphysics v5.5. 2020.
30. Xu, X.B.; Zhan, T.L.T.; Chen, Y.M.; Beaven, R.P. Intrinsic and relative permeabilities of shredded municipal solid wastes from the Qizishan landfill, China. *Can. Geotech. J.* **2014**, *51*, 1243–1252. [[CrossRef](#)]
31. Zhang, T.; Shi, J.; Qian, X.; Ai, Y. Temperature and gas pressure monitoring and leachate pumping tests in a newly filled MSW layer of a landfill. *Int. J. Environ. Res.* **2019**, *13*, 1–19. [[CrossRef](#)]
32. Shi, J.; Wu, X.; Ai, Y.; Zhang, Z. Laboratory test investigations on soil water characteristic curve and air permeability of municipal solid waste. *Waste Manag. Res.* **2018**, *36*, 463–470. [[CrossRef](#)]
33. Guerrero, J.S.P.; Pimentel, L.; Skaggs, T.H.; Van Genuchten, M.T. Analytical solution of the advection-diffusion transport equation using a change-of-variable and integral transform technique. *Int. J. Heat Mass Transf.* **2009**, *52*, 3297–3304. [[CrossRef](#)]